Flutter Analysis Using Nonlinear Aerodynamic Forces

T. Ueda* and E. H. Dowell†
Princeton University, Princeton, New Jersey

The nonlinear effects of transonic aerodynamic forces on the flutter boundary of a typical section airfoil are studied. The flutter speed dependence on amplitude is obtained by utilizing a novel variation of the describing function method which takes into account the first fundamental harmonic of the nonlinear oscillatory motion. By using an aerodynamic describing function, traditional flutter analysis methods may still be used while including the effects of aerodynamic nonlinearities. Results from such a flutter analysis are compared with those of brute force time-marching solutions. The aerodynamic forces are computed by the LTRAN2 aerodynamic code for an NACA 64A006 airfoil at $M_\infty = 0.86$.

Nomenclature

$A(\ ), A_L, A_M$ = indicial response functions
a = distance of elastic axis from midchord; percent semichord, positive downstream
b = semichord length
C_L^N = nonlinear lift coefficient
C_M^N = nonlinear moment coefficient about midchord
C_{Me}^N = nonlinear moment coefficient about elastic axis
c = full chord length
$\tilde{D}_L, \tilde{D}_M$ = components of describing function
F = output of describing function
G = structural transfer function
H = nonlinear aerodynamic transfer function
$\hat{H}$ = aerodynamic describing function
h = plunging displacement of elastic axis (positive down)
h_c = plunging displacement of midchord (positive down)
I_α = moment of inertia per unit span about elastic axis
k = reduced frequency, $c\omega/u$
L = lift force
M = moment force about midchord (positive nose-up)
M_∞ = Mach number of uniform airflow
m = mass per unit span
R = uncoupled frequency ratio, ω_h/ω_α
r_α = dimensionless radius of gyration about elastic axis (based on semichord); $r_\alpha^2 = r_{cg}^2 + (x_{cg} - a)^2$
r_{cg} = dimensionless radius of gyration about center of gravity (based on semichord)
S_α = static unbalance
s = dimensionless variable of Laplace operator; $s = ik$ for harmonic oscillation
t = time
U = dimensionless airspeed, $u/c\omega_\alpha\sqrt{\mu}$
u = dimensional airspeed
x_{cg} = distance of center of gravity from midchord; percent semichord, positive downstream
α = pitching displacement
μ = mass ratio, $m/\pi\rho b^2$
ρ = air density
τ = dimensionless time, ut/c
ϕ = effective induced angle of attack; see Eq. (1)
ϕ_1 = amplitude of ϕ oscillation
ω_h, ω_α = uncoupled circular frequency of the airfoil in plunging and in pitch, respectively

Superscripts

T = transpose of matrix
$\hat{(\ )}$ = quantity associated with describing function
$(\ )'$ = d/dt
$\bar{(\ )}$ = quantity in the subsidiary domain of Laplace operator

I. Introduction

RECENT developments in computational aerodynamics have led to renewed interest in the prediction of flutter boundaries of an airfoil in the transonic flow regime.[1-3] To date, flutter calculations have either assumed the transonic aerodynamic forces could be approximated as *linear* functions of the airfoil motion so that traditional *linear* flutter analysis methods could be used, or, alternatively, taken a brute force approach by simultaneously numerically integrating in time the structural and aerodynamic equations. The latter method does, of course, fully account for aerodynamic nonlinearities.

Ballhaus and Goorjian[1] calculated the aeroelastic response of an NACA 64A006 airfoil with a single-degree-of-freedom control surface by simultaneously integrating numerically in time the structural equation of motion and the aerodynamic equations. They used their own code, LTRAN2, for unsteady transonic flow. The indicial method, whereby an aerodynamic impulse function is first calculated by the aerodynamic code and then used in the flutter calculation via a convolution integral, was also studied. The indicial method assumes linearity of the aerodynamic forces with respect to airfoil motion. The flutter of the same airfoil, but with two degrees of freedom, was analyzed by Yang et al.[2] with aerodynamic forces obtained by three different methods. These forces were obtained by the time-integration method, the indicial method

Presented as Paper 82-0728 at the AIAA/ASME/ASCE 23rd Structures, Structural Dynamics, and Materials Conference, New Orleans, La., May 10-12, 1982; submitted May 28, 1982; revision received Sept. 13, 1983.

*Visiting Scholar, Department of Mechanical and Aerospace Engineering; presently Research Engineer, National Aerospace Laboratory, Tokyo, Japan. Member AIAA.

†Professor, Department of Mechanical and Aerospace Engineering; now, Dean of Engineering, Duke University, Durham, N.C. Associate Fellow AIAA.

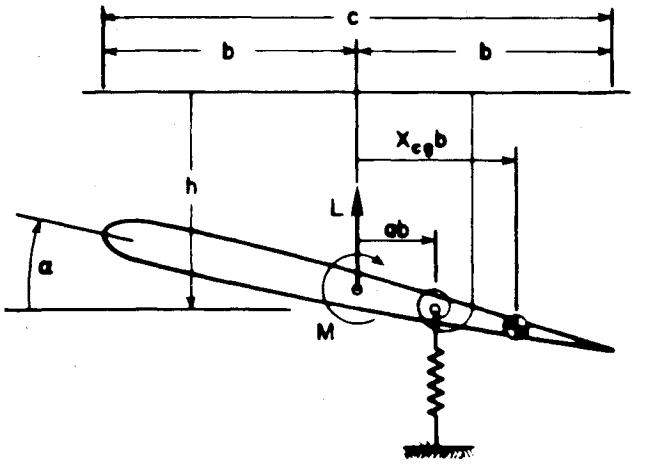

Fig. 1 Typical section airfoil.

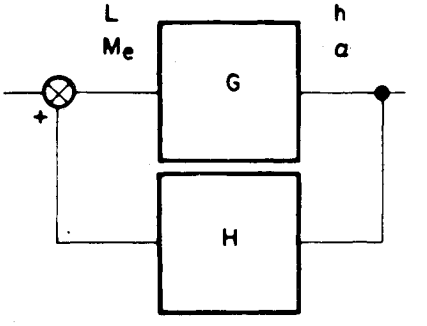

Fig. 2 Block diagram of typical section airfoil system.

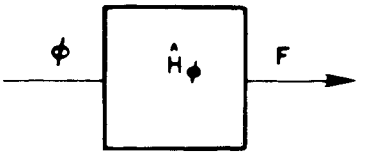

Fig. 3 Aerodynamic describing function.

(both of these employed the LTRAN2 code), and the harmonic analysis method in the frequency domain using the UTRANS2 code. The latter method also assumes linearity of the aerodynamic forces. In general, all three methods agree well for the range of parameters studied by Yang. After the flutter boundary was obtained, the response was confirmed near the flutter boundary by simultaneous time integration of the governing structural and aerodynamic equations. Isogai[3] studied the transonic behavior of the NACA 64A010 airfoil by using his own USTS transonic aerodynamic code which can be applied to supercritical Mach numbers for reduced frequencies, $0<k<1.0$. (By contrast, the aerodynamic methods used by Yang were limited to small k.) Isogai used the time-integration method for evaluating the aerodynamic forces, but then converted them to linearized harmonic forces for the flutter calculations. See Yang et al.[4] for further discussion of previous work on flutter calculations, including other investigators who have used brute force, simultaneous numerical integration of the structural and aerodynamic equations.

A discussion of when the aerodynamic forces may be treated as linear in the airfoil motion is given in Ref. 5. The analyses of Refs. 2 and 3 described above assumed linear characteristics for the aerodynamic forces in the flutter calculations. Linearity can be assured if the amplitude of the airfoil oscillation is sufficiently small,[5] even though the governing fluid equations are inherently nonlinear for transonic flowfields. Yang et al.[2] fixed an amplitude of pitching motion at 0.01 rad (0.574 deg), whereas Isogai[3] used 0.1 in degrees for the computation of the aerodynamic forces. Dowell et al.[5] pointed out that increasing the value of the reduced frequency increases the range of amplitude of oscillation for which linear behavior exists in transonic flow. However, the aerodynamic forces often begin to deviate from linear behavior for amplitudes of relatively small value, such as 1.0 deg in pitching motion. Such amplitudes may be attained due to the disturbances an aircraft wing encounters during its flight. It is of importance, therefore, to clarify the aerodynamic nonlinear effect on a flutter boundary, especially when the nonlinear effect may create an aeroelastic softening system, i.e., the flutter speed decreases as the amplitude of oscillation increases. Such softening behavior may cause a dangerous unconservative estimation of a flutter boundary by linear analysis.

Herein we study the nonlinear effect of transonic aerodynamic forces on a flutter boundary by utilizing a novel variation of the describing function method,[6] which takes into account the first fundamental harmonic of the nonlinear oscillatory motion. By using an aerodynamic describing function, traditional flutter analysis methods may still be used while *including* (approximately) the effects of aerodynamic nonlinearities. Brute force time-marching calculations are also done for comparison purposes.

The method used to calculate the describing functions is briefly outlined as follows. A step change in angle of attack is specified and the transient aerodynamic force time history (calculated numerically by an appropriate aerodynamic code) is identified as a nonlinear impulse function. The Fourier transform of this impulse function (which in general depends upon the step input level or amplitude) is taken as the aerodynamic describing function. Calculations have shown that this describing function agrees very well with the one determined by using a harmonic angle of attack input to the aerodynamic code. The latter method of calculation is, of course, much more expensive and time consuming for the range of frequencies needed in flutter analysis. The LTRAN2 computer code is used for determining the aerodynamic forces. However any other nonlinear code could be used in a similar fashion.

II. Typical Airfoil Section

A typical section airfoil subjected to transonic flow is considered as shown in Fig. 1. This system is characterized mathematically by the block diagram depicted in Fig. 2 where G and H are the structural and aerodynamic transfer functions, respectively.

Since it can be assumed that the structural deformation is linearly dependent on the aerodynamic load for wings of ordinary modern aircraft during its normal flight, a *linear* structural transfer function is used. The aerodynamic forces, however, may depend in a nonlinear manner on the structural deformation in the transonic flow range.[5] In order to include the nonlinear effect of large(r) amplitudes of motion on the aerodynamic forces and, hence, on a flutter boundary, we use a *nonlinear* aerodynamic transfer function by employing the describing function method.

III. Aerodynamic Describing Function

Herein we give a summary of the relevant standard describing function results and place the present method in context.

If we assume that the frequency of motion is relatively low, the aerodynamic forces due to the airfoil motion can be approximated as a function of the effective induced angle of

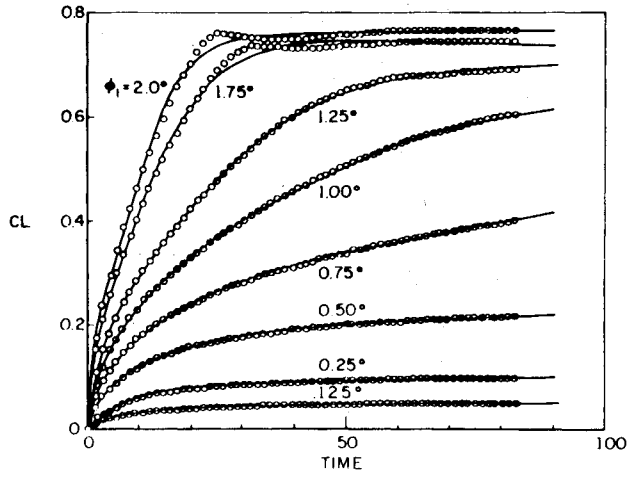

Fig. 4a Indicial responses computed by LTRAN2 and exponential curve fit, lift.

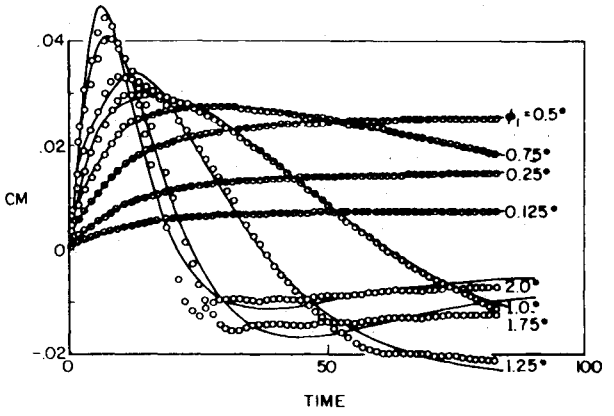

Fig. 4b Indicial responses computed by LTRAN2 and exponential curve fit, moment.

attack which is given by

$$\phi = \alpha + (\dot{h}_c/u) \tag{1}$$

This quasisteady approximation is compatible with the low-frequency assumption in the LTRAN2 transonic unsteady aerodynamic code which we use in the present flutter calculation. Taking into account the nonlinear effects of the amplitudes of motion, we assume the aerodynamic forces in the form:

$$L = \tfrac{1}{2}\rho u^2 c C_L^N(\phi,\dot{\phi}) \tag{2}$$

$$M = \tfrac{1}{2}\rho u^2 c^2 C_M^N(\phi,\dot{\phi}) \tag{3}$$

where C_L^N, C_M^N are functionals of $\phi,\dot{\phi}$, i.e., they may, in principle, include the complete time history of ϕ and $\dot{\phi}$.

For general periodic time-dependent motion, the effective angle of attack ϕ can be expanded in a Fourier series as

$$\phi = \frac{\phi_0}{2} + \sum_n^N \left[\phi_{I,n}\cos(nk\tau) + \phi_{R,n}\sin(nk\tau)\right] \tag{4}$$

According to the describing function method only the first harmonic of ϕ is taken as an input to the aerodynamic force transfer function, i.e.,

$$\phi = \phi_I \sin k\tau \tag{5}$$

This input motion generates aerodynamic forces through the nonlinear element H which, in general, include higher harmonics. Thus,

$$C_L^N(\phi,\dot{\phi}) = \frac{C_{L_{I,0}}(\phi_I)}{2} + \sum_n^N [C_{L_{I,n}}(\phi_I)\cos(nk\tau) + C_{L_{R,n}}(\phi_I)\sin(nk\tau)] \tag{6}$$

$$C_M^N(\phi,\dot{\phi}) = \frac{C_{M_{I,0}}(\phi_I)}{2} + \sum_n^N [C_{M_{I,n}}(\phi_I)\cos(nk\tau) + C_{M_{R,n}}(\phi_I)\sin(nk\tau)] \tag{7}$$

The describing function method, however, replaces the nonlinear element H by another nonlinear element $\hat{H}$ with the property that it operates on any sinusoidal input, Eq. (5), by passing its fundamental frequency in exactly the same manner as H; however, whatever the input frequency k, $\hat{H}$ generates no higher harmonics. This replacement allows us to write

$$\hat{C}_L^N(\phi,\dot{\phi}) = C_{L_{I,1}}(\phi_I)\cos(k\tau) + C_{L_{R,1}}(\phi_I)\sin(k\tau) = D_{L_R}(\phi_I)\phi + D_{L_I}(\phi_I)\dot{\phi}/k \tag{8}$$

$$\hat{C}_M^N(\phi,\dot{\phi}) C_{M_{I,1}}(\phi_I)\cos(k\tau) + C_{M_{R,1}}(\phi_I)\sin(k\tau) = D_{M_R}(\phi_I)\phi + D_{M_I}(\phi_I)\dot{\phi}/k \tag{9}$$

where

$$D_{L_R} = \frac{1}{\pi\phi_I}\int_0^{2\pi} C_L^N(\phi,\dot{\phi})\sin(k\tau)\mathrm{d}(k\tau) \tag{10}$$

$$D_{L_I} = \frac{1}{\pi\phi_I}\int_0^{2\pi} C_L^N(\phi,\dot{\phi})\cos(k\tau)\mathrm{d}(k\tau) \tag{11}$$

$$D_{M_R} = \frac{1}{\pi\phi_I}\int_0^{2\pi} C_M^N(\phi,\dot{\phi})\sin(k\tau)\mathrm{d}(k\tau) \tag{12}$$

$$D_{M_I} = \frac{1}{\pi\phi_I}\int_0^{2\pi} C_M^N(\phi,\dot{\phi})\cos(k\tau)\mathrm{d}(k\tau) \tag{13}$$

Using complex notation for Eqs. (8) and (9) yields a more compact result, i.e.,

$$\hat{C}_L^N(\phi,\dot{\phi}) = D_{L_I}(\phi_I)\phi \tag{14}$$

$$\hat{C}_M^N(\phi,\dot{\phi}) = D_{M_I}(\phi_I)\phi \tag{15}$$

where

$$D_{L_I}(\phi_I) = D_{L_R} + iD_{L_I} \tag{16}$$

$$D_{M_I}(\phi_I) = D_{M_R} + iD_{M_I} \tag{17}$$

In Eqs. (14) and (15), the coefficients $\hat{C}_L^N$ and $\hat{C}_M^N$ also have complex values whose real parts correspond to Eqs. (8) and (9), respectively.

If the amplitude ϕ_I is fixed, then Eqs. (14) and (15) take a form identical to that for a linear system. This implies the applicability of the same stability analysis as that for a linear system.

The coefficients defined in Eqs. (10-13) to construct the describing function can be computed by the time-integration code for transonic flow. It is also possible to evaluate them from wind tunnel experimental data measured on a harmonically excited airfoil. In the present study we utilize an *extended nonlinear* version of the indicial method[1] to calculate the aerodynamic coefficients.

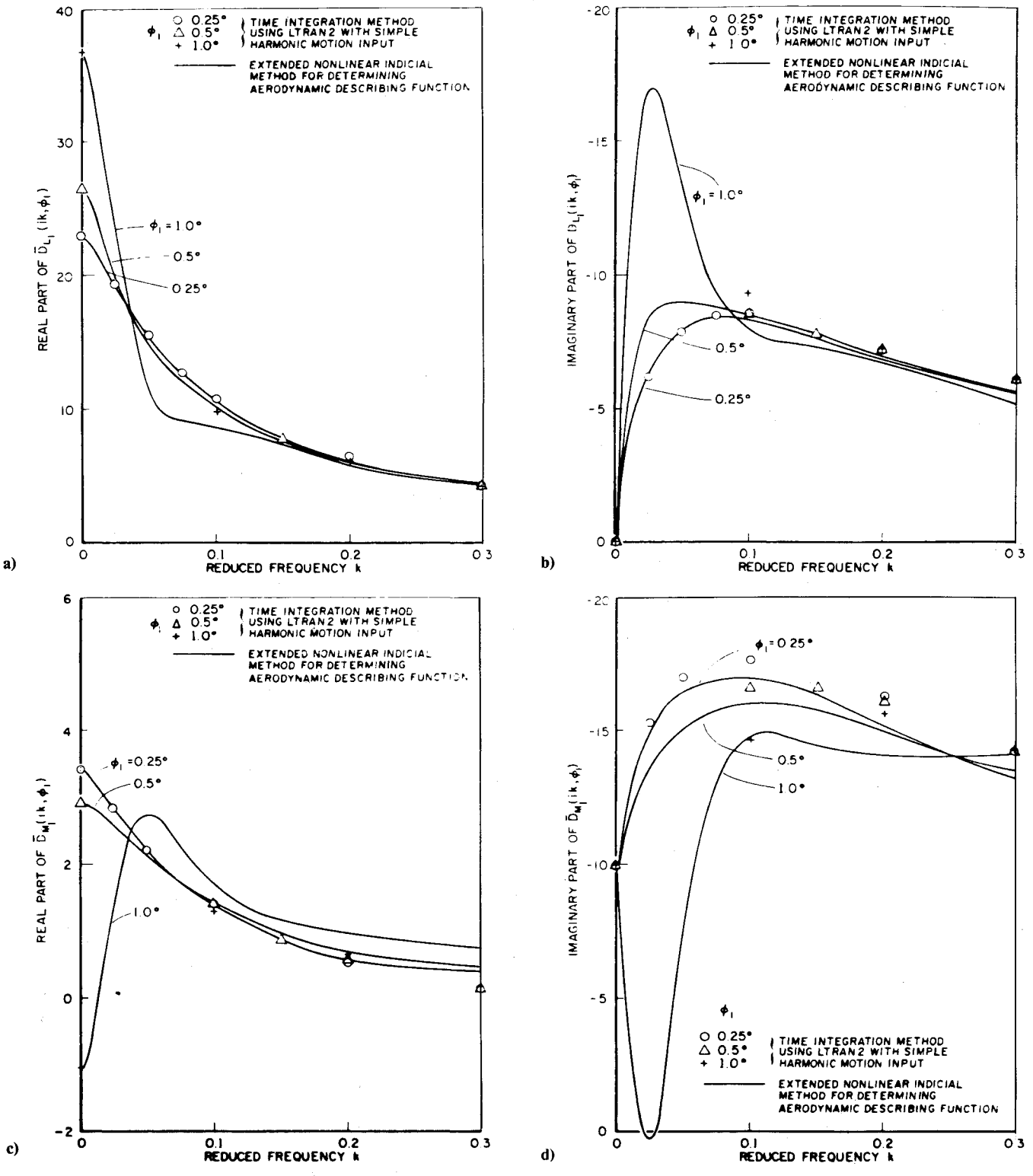

Fig. 5 Comparison of extended nonlinear indicial method with time-integration method (NACA 64A006, $M_\infty = 0.86$).

Since the describing function assumes the same form as a linear transfer function when the amplitude is fixed, we can regard the element $\hat{H}_\phi$ (shown in Fig. 3) as a linear system *with respect to variations in frequency.*

$$F(\tau) = \hat{H}_\phi(ik,\phi_1)\,\phi_1 e^{ik\tau} \tag{18}$$

This relation corresponds in the subsidiary (effectively frequency) domain of the Laplace operator to the following:

$$\bar{F}(s) = \hat{H}(s,\phi_1)\,\frac{\phi_1}{s-ik} \tag{19}$$

If we put $k=0$, then Eq. (19) represents an indicial response relationship.

$$\bar{\hat{A}}(s,\phi_1) = \hat{H}_\phi(s,\phi_1)\,\frac{\phi_1}{s} \tag{20}$$

By using Eq. (20) we can obtain the describing function, $\hat{H}_\phi(ik,\ \phi_1)$, from the indicial response to a step input with amplitude ϕ_1. Furthermore, if we neglect the effect of higher harmonics, an assumption already made in the describing function method, then $\hat{H}_\phi(ik,\ \phi_1)$ can be approximated by

Table 1 Comparison of flutter solution results

	ϕ_1, deg	$u/b\omega_\alpha$	k_F
Present method	0.125	3.42	0.128
	0.25	3.43	0.128
	0.5	3.48	0.125
	1.0	3.69	0.124
Yang et al.[9]	Indicial		
	method	3.60	0.135
	Relaxation	3.89	0.105
Classical subsonic			
Linear theory		3.89	0.130

(NACA 64A006, $M_\infty = 0.86$, $a = -0.5$, $x_{cg} = 0.0$, $r_{cg}^2 = 0.0$, $R = 0.1$, $\mu = 100$.)

using the indicial response $\bar{A}(s,\phi_1)$ of the element H as

$$\hat{H}_\phi(ik,\phi_1) = \bar{A}(ik,\phi_1)\, ik/\phi_1 \tag{21}$$

For a linear system, starting from Eq. (18) one may proceed through Eqs. (19-21) and vice versa by standard mathematical methods. However, as the careful reader will note, this is not strictly possible for a nonlinear system, i.e., Eqs. (19) and (20) follow from Eq. (18) only *by analogy* to linear system results. Indeed we may take Eqs. (18) and (21) [or Eq. (20)], as two *independent* definitions of $\hat{H}(ik,\phi_1)$, the describing function which will be used in the flutter analysis. However, by numerical example, we will show that, in fact, the two definitions lead to similar results. This is fortunate, because the less obvious definition, Eq. (21), is far easier to use in practice for generating aerodynamic forces to employ in flutter calculations.

IV. Working Form of the System Equations

The governing structural equations of the system are given in nondimensional form by

$$\frac{\pi\mu}{2}\left(\frac{h}{c}\right)'' + \frac{\pi\mu}{2}\left(\frac{S_\alpha}{mc}\right)\alpha'' + \frac{\pi\mu}{2}\left(\frac{c\omega_h}{u}\right)^2\left(\frac{h}{c}\right) = -C_L^N \tag{22}$$

$$\frac{\pi\mu}{2}\left(\frac{S_\alpha}{mc}\right)\left(\frac{h}{c}\right)'' + \frac{\pi\mu}{2}\left(\frac{I_\alpha}{mc^2}\right)\alpha'' + \frac{\pi\mu}{2}\left(\frac{I_\alpha}{mc^2}\right)\left(\frac{c\omega_\alpha}{u}\right)^2\alpha = C_{Me}^N \tag{23}$$

From Eqs. (22) and (23), the structural transfer function for the state vector, $[(h/c)\alpha]^T$, is

$$G^{-1}(s,U) = \begin{bmatrix} \frac{\pi}{2}\{\mu s^2 + R^2/U^2\} & \frac{\pi\mu}{4}(x_{cg}-a)s^2 \\ \frac{\pi\mu}{4}(x_{cg}-a)s^2 & \frac{\pi}{8}r_\alpha^2\{\mu s^2 + 1/U^2\} \end{bmatrix} \tag{24}$$

As to the aerodynamic describing function, we first assume the indicial response $A(\tau,\phi_1)$ to a step change in ϕ [Eq. (21)] can be expressed in the following form for the lift and moment forces:

$$A_L(\tau,\phi_1) = a_0^L(\phi_1) + \sum_{i=1}^{N} a_i^L(\phi_1)\, e^{b_i^L \tau} \tag{25}$$

$$A_M(\tau,\phi_1) = a_0^M(\phi_1) + \sum_{i=1}^{N} a_i^M(\phi_1)\, e^{b_i^M \tau} \tag{26}$$

where a_0^L and a_0^M are chosen to be identical to the steady-state

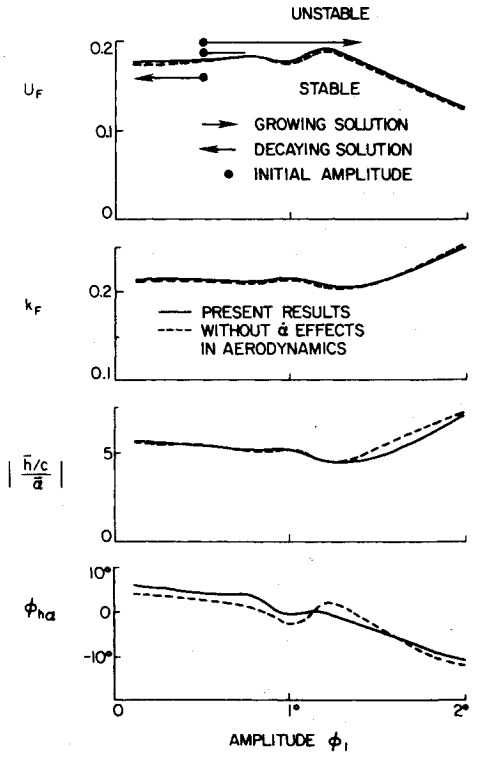

Fig. 6 Flutter boundaries vs amplitudes; NACA 64A006, $M_\infty = 0.86$, $a = -0.3$, $x_{cg} = 0.2$, $r_{cg}^2 = 0.24$, $R = 0.2$, $\mu = 60$.

values for $\phi = \phi_1$, since every b_i is chosen to be a negative real number. The coefficients a_i^L, a_i^M are determined by the least-square method for fixed values of b_i. The b_i are selected to be in the vicinity of the negative of the k values for which the imaginary parts of the aerodynamic transfer function have extrema. This procedure for selecting the b_i is discussed in detail in Ref. 7.

After determining the coefficients in Eqs. (25) and (26), the indicial response functions can be written in the subsidiary domain of the Laplace operator (frequency domain) as

$$\bar{A}_L(s,\phi_1) = \frac{a_0^L}{s} + \sum_{i=1}^{N} \frac{a_i^L}{s - b_i^L} \tag{27}$$

$$\bar{A}_M(s,\phi_1) = \frac{a_0^M}{s} + \sum_{i=1}^{N} \frac{a_i^M}{s - b_i^M} \tag{28}$$

Then, from Eq. (21), the aerodynamic describing function is obtained for the state variable ϕ as

$$\hat{H}_\phi(ik,\phi_1) = [\bar{D}_L(ik,\phi_1)\, \bar{D}_M(ik,\phi_1)]^T \tag{29}$$

where

$$\bar{D}_L(ik,\phi_1) = ik\bar{A}_L(ik,\phi_1)/\phi_1 \tag{30}$$

$$\bar{D}_M(ik,\phi_1) = ik\bar{A}_M(ik,\phi_1)/\phi_1 \tag{31}$$

In order to construct the aerodynamic describing functions so that they are compatible with the structural transfer function, we must transform ϕ and C_M^N to those variables used in the structural equations of motion. The relationships for the state vectors and the moment coefficients are as follows:

$$\bar{\phi}(ik) = \left(ik\, 1 - \frac{a}{2}ik\right)\begin{bmatrix} \overline{h/c} \\ \alpha \end{bmatrix} \tag{32}$$

$$C_{Me}^N = C_M^N + \frac{a}{2}C_L^N \tag{33}$$

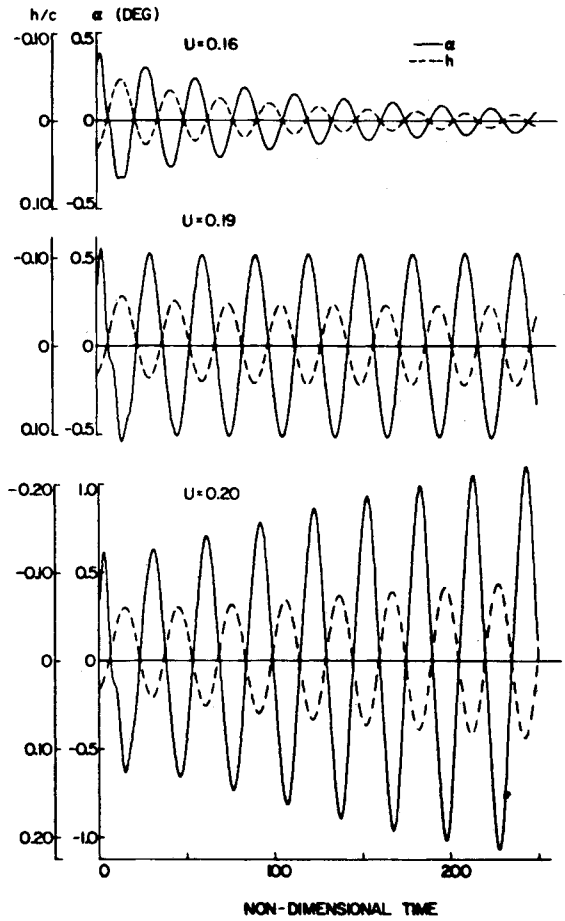

Fig. 7 Time history of time-marching solutions.

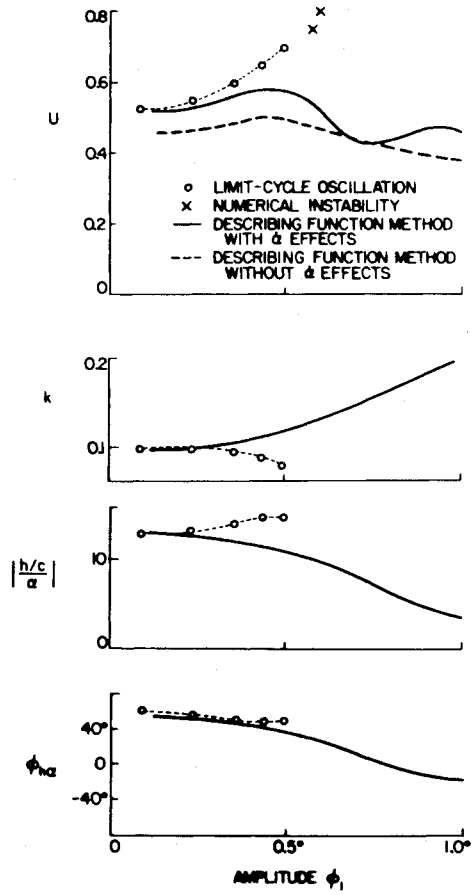

Fig. 8 Limit cycle oscillations; NACA 64A006, $M_\infty = 0.86$, $\alpha = -0.3$, $x_{cg} = -0.25$, $r_{cg}^2 = 0.24$, $R = 0.1$, $\mu = 60$.

As the aerodynamic describing function $\hat{H}(ik,\phi_1)$ is defined by

$$\begin{bmatrix} -\bar{C}_L^N(ik,\phi_1) \\ \bar{C}_{Me}^N(ik,\phi_1) \end{bmatrix} = \hat{H}(ik,\phi_1) \begin{bmatrix} \bar{h}/c \\ \alpha \end{bmatrix} \tag{34}$$

using Eqs. (30-34), it becomes

$$H(ik,\phi_1) = \begin{bmatrix} A_{11} & A_{12} \\ A_{21} & A_{22} \end{bmatrix} \tag{35}$$

where

$$A_{11} = -\bar{D}_{L_1}(ik,\phi_1)ik$$

$$A_{12} = -\bar{D}_{L_1}(ik,\phi_1)\left(1-\frac{a}{2}ik\right)$$

$$A_{21} = \bar{D}_{L_1}(ik,\phi_1)\frac{a}{2}ik + \bar{D}_{M_1}(ik,\phi_1)ik$$

$$A_{22} = \bar{D}_{L_1}(ik,\phi_1)\frac{a}{2}\left(1-\frac{a}{2}ik\right) + \bar{D}_{M_1}(ik,\phi_1)\left(1-\frac{a}{2}ik\right)$$

$$= D_{L_R}(\phi_1)\phi + D_{L_I}(\phi_1)\dot{\phi}/k$$

Using the structural transfer function, Eq. (24), and the aerodynamic describing function, Eq. (35), a self-sustained oscillation of the system shown in Fig. 2 is characterized by the equation

$$|G^{-1}(ik,U) - \hat{H}(ik,\phi_1)| = 0 \tag{36}$$

Equation (36) corresponds to the so-called flutter determinant if the system is linear. For the present nonlinear system, Eq. (36) allows one to determine the amplitude of the flutter motion as a function of some system parameter, say airspeed. speed.

V. Extension of the Describing Function

In Sec. III, we assumed the aerodyanamic forces can be given as functions of a single variable, ϕ. More rigorously, however, the upwash of the mean camber line of an airfoil is given by

$$-\frac{w}{u} = \phi + \frac{c\dot{\alpha}}{u}(x/c - 0.5) \tag{37}$$

where the airfoil is located on $0 \leqq x \leqq c$. The second term in Eq. (37) includes the effect of the angular velocity of the airfoil motion, $\dot{\alpha}$. If we take into account this aerodynamic effect in the flutter analysis, the aerodynamic describing function must be determined separately for h and α motion, or alternatively for ϕ and $\dot{\alpha}$. Moreover, this procedure makes the describing function method less obvious as to its theoretical basis. Neglecting the effect of $\dot{\alpha}$, however, we encountered fictitious instabilities at high frequencies, as well as a decrease of flutter speeds. To eliminate this artifact, an improvement was made to the aerodynamic describing function by adding the component that is derived from the second term of Eq. (37). This is based on the assumption that the $\dot{\alpha}$ effect compared to ϕ is generally secondary for the aerodynamic forces at low reduced frequencies, k, where

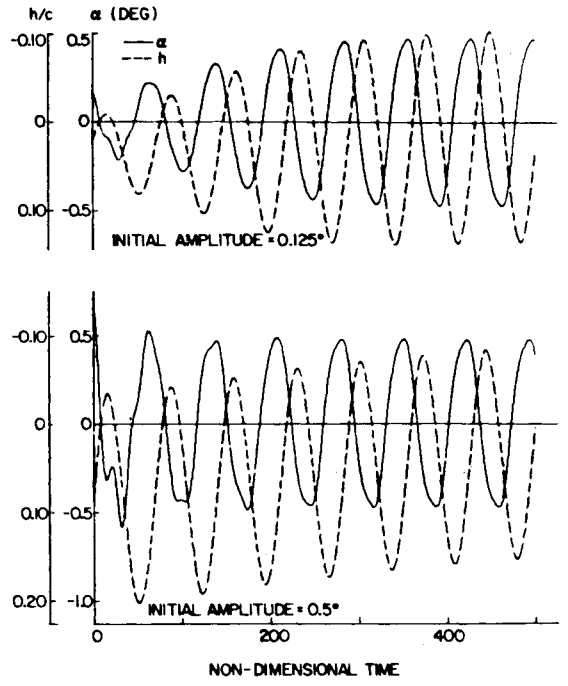

Fig. 9 Time history of limit cycle flutter; $U=0.6$, $\phi_I=0.355$ deg, $k_F=0.089$, $|(\bar{h}/c)/\bar{\alpha}|=14.4$, $\phi_{h\alpha}=49.7$ deg.

nonlinear transonic aerodynamic effects are most significant. Thus, the components of the describing function, Eq. (35), are redefined by

$$A_{12}=A_{12}-\bar{D}_{L_2}(ik)ik$$
$$A_{22}=A_{22}+\bar{D}_{L_2}(ik)\frac{a}{2}ik+\bar{D}_{M_2}(ik)ik \tag{38}$$

where A_{12} and A_{22} on the right-hand side of Eq. (38) are those of Eq. (35). $\bar{D}_{L_2}$ and $\bar{D}_{M_2}$ are the components obtained from an indicial response of the second term of Eq. (37). For brevity, details are omitted.

VI. Results and Discussions

Aerodynamic Results

All of the original aerodynamic data in the following were computed by the LTRAN2[8] code for an NACA 64A006 airfoil with Mach number set to $M_\infty=0.86$ where characteristically transonic effects can be observed. Results were also calculated for an NACA 64A010 airfoil, but these are omitted here. The zero-angle-of-attack, steady-state shock stands roughly at midchord.[5] In this calculation a 113×97 finite difference mesh was employed. The nondimensional time increment, $\Delta\tau$, for integration was selected at $\pi/12$ to obtain indicial responses. The lift and moment forces at every five time increments were used to evaluate the coefficients in Eqs. (25) and (26). In order to compare the aerodynamic forces with those obtained by the present extended nonlinear indicial method, the time integration for the airfoil undergoing harmonic excitation of pitching motion about midchord axis was also performed with 120 time steps per cycle at various reduced frequencies. The latter results [using Eq. (18)] were compared to those obtained by the indicial method using the Laplace transform versions of Eqs. (25) and (26) which derive from Eq. (21). In general, good agreement was obtained.

The indicial response to step functions of different amplitudes, ϕ_I, are shown in Fig. 4. Generally, in this type of indicial response, a spike should appear near $\tau=0$. However, the low-frequency theory of LTRAN2 can not follow a piston-wave-type pressure change because of its infinite propagation rate.[1] Hence, in the present calculations the lift coefficient increases gradually from zero at $\tau=0$.

In the results of Fig. 4, the curves prescribed by Eqs. (25) and (26) are also shown after the coefficients were determined by the least-square method using 64 time data points for the indicial response at each amplitude. b_i^L and b_i^M are selected at six values ($N=6$): -0.01875, -0.0375, -0.075, -0.15, -0.3, and -0.6. These results, obtained from Eqs. (25) and (26), are in excellent agreement with the indicial responses computed by the LTRAN2 code, especially for the lower amplitude values of step inputs. Using the coefficients a_i^L, a_i^M, and Eq. (21) we can obtain the elements of the aerodynamic functions, $\bar{D}_{L_I}(ik,\phi_I)$ and $\bar{D}_{M_I}(ik,\phi_I)$ as shown in Fig. 5. They are plotted for reduced frequencies up to 0.3. Although the describing function for higher frequencies can be calculated by Eqs. (30) and (31), they are no longer meaningful at those frequencies because of the low-frequency limitation[8] in LTRAN2.

In Fig. 5, the describing functions thus obtained are also compared with the results of the time-integration method for simple harmonic motion inputs which use Eqs. (10-13) [also see Eq. (18)]. The agreement between the two methods is generally satisfactory. However, it is seen that the agreement is better for smaller rather than larger amplitude, for lift rather than for moment, and for real part rather than for imaginary part. It should be emphasized that the extended nonlinear indicial method has substantially greater simplicity and efficiency, as compared to the time-integration method for simple harmonic motion inputs, in determining the aerodynamic describing function.

Flutter Results

Some flutter calculations have been done using these aerodynamic describing functions for typical section airfoils. First, the parameters of a typical section airfoil were chosen to compare with the results by Yang et al.[9] A comparison is made in Table 1. The flutter boundary calculated by the present method for an amplitude ϕ_I between 0.5 and 1.0 deg agrees well with that obtained from the *linear* indicial method by Yang et al.

To investigate the *amplitude* effect on the flutter boundary, a typical section airfoil corresponding to case B in Ref. 3 was considered next, although the results cannot be compared directly with those in Ref. 3 due to the use of a different airfoil profile. The results of the flutter speed, as well as of the reduced-frequency, bending/torsion amplitude ratio and phase, are shown in Fig. 6. Those without the $\dot{\alpha}$ effect are depicted by dashed curves. In this case, the effect of angular velocity on flutter boundaries was very small.

As the aerodynamic describing function method invokes several assumptions, a fully nonlinear time-marching solution was computed to verify the above results. The numerical integration scheme adopted for structural equations is the state transition matrix method which Edwards et al.[10] recommended after examining seven different integrators for a similar calculation (see Refs. 10, 12).

Three time-marching calculations with different speed parameters have been carried out for the case shown in Fig. 6. The initial state vector was determined from the flutter solution of the describing function method with $\phi_I=0.5$ deg, namely, $U_F=0.1798$, $k_F=0.2126$, $|(\bar{h}/c)/\bar{\alpha}|=5.446$, and $\phi_{h\alpha}=4.24$ deg. If we choose the initial time, $\tau=0$, as the instant when $\dot{\alpha}=0$, the flutter solution gives the initial state vector for the time marching as $x=(0.03164,\ 0.00583,\ -0.00049,\ 0)^T$. The time increment for integration was selected as $\Delta\tau=0.25$ which, when considering the flutter reduced frequency, corresponds roughly to 120 steps per cycle. Although the initial state vector is determined from the describing function flutter motion, the time marching is started from a steady-state initial condition of the airfoil at a static angle of attack for the aerodynamic calculations. For example, the initial effective induced angle of attack becomes

0.305 deg for this case. It should be noted that the second term of Eq. (37) vanishes at the initial upwash, since the starting time is set at the instant when the angular velocity becomes zero. The time marching is continued up to $\tau=250$, which contains 1000 time steps. The variations of the amplitude ϕ_l of these solutions are shown in Fig. 6 and the time histories in Fig. 7. At $U=0.16$, the airfoil shows decaying motion, whereas the oscillation is growing at $U=0.2$. At $U=0.19$, the oscillation is almost neutral although it is slightly growing. The changes of the peak values in the effective angle of attack of these oscillations are illustrated in Fig. 6. The solid curve shows the flutter boundary obtained by the describing function method. In this case, the flutter boundary is nearly horizontal at small amplitudes. As can be seen from the figure, the results from the describing function method agree well with those of the time-marching solution. Furthermore, the last cycle of the time-marching solution at $U=0.19$ gives the values of $\phi_l=0.723$, $k=0.212$, $|(\bar{h}/c)/\bar{\alpha}|=5.18$, and $\phi_{h\alpha}\simeq 5$ deg. The agreement of these values with the results in Fig. 6 is excellent. It should be noted that the damping in the time-marching solutions is attributed to the aerodynamic forces since we use no structural damping nor artificial damping due to numerical integration schemes. It is known that the transition matrix integrator gives exactly neutral solutions for free structural vibration, irrespective of its time step size.

Since the nonlinear effect is most important at relatively *low* reduced frequencies (see Fig. 5), the center of gravity was next placed at $x_{cg}=-0.25$ and the frequency ratio at $R=0.1$ in order to obtain a distinctly nonlinear effect. The results are shown in Fig. 8. On those portions of the curve where amplitude increases with airspeed, a stable nonlinear limit cycle is predicted. On those portions of the curve where amplitude increases with *decreases* in airspeed, an unstable limit cycle occurs.

Further time-marching calculations have been performed to confirm the limit cycle. The initial state vector to start time integrations is varied proportionally to that of the flutter solution of the describing function method with the amplitude $\phi_l=-0.25$ deg, which gives $x=(0.04353,\ 0.00562,\ -0.005726,\ 0)^T$ for $\phi_l=0.25$ deg. This state vector yields the effective induced angle of attack, -0.0063 deg, at $\tau=0$. Since the reduced frequencies of flutter are about 0.1 for small amplitudes, the time step size of integration was chosen as $\Delta\tau=0.5$.

As the solid curve of the describing function in Fig. 8 anticipates, the limit cycle flutter is also shown by the time-marching solutions for small amplitudes. The amplitudes, reduced frequencies, amplitude ratio, and phase angles of these limit cycle oscillations were also calculated from the time history of the solutions and are depicted with open circles in the figure. Convergence to the limit cycle is determined by changing the initial amplitude. For example, the time history with two different initial amplitudes at $U=0.6$ is shown in Fig. 9. Both oscillations converge to the same limit cycle with the amplitude $\phi_l=0.355$ deg beyond $\tau=400$. However the average displacement for the h motion at least up to $\tau=500$ is different for the two initial conditions. This slow convergence for the average displacement to the neutral position may be attributed to the small frequency ratio R, which implies weak stiffness of the structure against the h motion. It should be noted that the *average* translational displacement of an airfoil has no effect on the aerodynamic forces.

The results of the time-marching solution can be compared with those obtained by the describing function method in Fig. 8. For small amplitudes, the agreement of the results is satisfactory. The reduced frequency of the limit cycle by the time-marching solution, however, decreases as the flutter amplitude increases, while the describing function method predicts monotonically increasing reduced frequencies. Further, the time-marching solution shows stable limit cycle flutter up to the speed of $U=0.7$, whereas the describing function method predicts no stable limit cycle solution above $U=0.58$. At $U=0.75$ and 0.8, the time-marching solutions with the initial amplitude of $\phi_l=0.5$ deg, are terminated by a *numerical* instability of the aerodynamic calculations. The peak values of ϕ just before the occurrence of the instability are plotted with the symbol $\times$. This kind of difficulty was frequently encountered when we used an initial amplitude of more than 0.5 deg in the time-marching calculations. *Possibly* for this reason we failed to detect the divergent unstable limit cycle flutter with larger amplitudes which is predicted by the describing function method.

VII. Concluding Remarks

An extended nonlinear indicial approach to modeling nonlinear aerodynamic forces for aeroelastic analyses has been developed. The basic approach is based upon describing function ideas.

The flutter boundaries obtained by the describing function method are generally verified by time-marching solutions for sufficiently small-amplitude flutter motion. Hence, the former, less costly method is useful for determining the significance of initial departures from linear behavior. More specific conclusions are as follows.

1) Generally the accuracy of the describing function method decreases as the amplitude of the motion increases. However, the describing function method is a powerful tool to predict the characteristics of transonic flutter, since it requires a very small amount of computation time for the aerodynamic forces compared to time-marching solutions.

2) The stable nonlinear limit cycle flutter predicted by the describing function method is also observed in the time-marching solutions.

3) The component in the upwash distribution due to the angular velocity $\dot{\alpha}$ airfoil motion cannot always be neglected even though the aerodynamic code has a low-frequency limitation. Sometimes its neglect causes a fictitious flutter instability of the α motion at high frequencies.

4) The $\dot{\alpha}$ effect is properly taken into account by the total describing function decomposition into ϕ and $\dot{\alpha}$ components.

5) The nonlinear behavior with the large amplitudes, $\phi>0.5$ deg, could not be obtained by the time-marching solutions due to a numerical instability in the aerodynamic calculations (even when $\dot{\alpha}$ effects are included).

For an alternative suggestion for achieving the same goals, the reader is directed to Ref. 11; also, the recent work of Bland and Edwards[12] should be cited. They deal with the important effects of airfoil shape and thickness (although not nonlinear dynamic effects per se) in a manner similar to that of the present paper.

Acknowledgments

This work is supported by AFOSR Grant 81-0123. Dr. Anthony Amos is the Technical Monitor.

References

[1] Ballhaus, W.F. and Goorjian, P.M., "Computation of Unsteady Transonic Flows by the Indicial Method," *AIAA Journal,* Vol. 16, Feb. 1978, pp. 117-124.

[2] Yang, T.Y., Guruswamy, P., and Striz, A.G., "Aeroelastic Response Analysis of Two Dimensional, Single and Two Degree of Freedom Airfoils in Low Frequency, Small-Disturbance Unsteady Transonic Flow," AFFDL-TR-79-3077, 1979.

[3] Isogai, K., "Numerical Study of Transonic Flutter of a Two-Dimensional Airfoil," National Aerospace Laboratory, Japan, Tech. Rept. NAL-TR-617T, 1980.

[4] Yang, T.Y., Guruswamy, P., and Striz, A.G., "Application of Transonic Codes to Flutter Analysis of Conventional and Supercritical Airfoils," *Proceedings of the 22nd AIAA/SDM Conference,* Atlanta, Ga., 1981.

[5] Dowell, E.H., Bland, S.R., and Williams, M.H., "Linear/Nonlinear Behavior in Unsteady Transonic Aerodynamics," *AIAA Journal,* Vol. 21, Jan. 1983, pp. 38-46.

[6] Hsu, J.C. and Meyer, A.U., *Modern Control Principles and Applications,* McGraw-Hill, New York, 1968.

[7]Dowell, E.H., "A Simple Method for Converting Frequency-Domain Aerodynamics to the Time Domain," NASA TM 81844, 1980.

[8]Ballhaus, W.F. and Goorjian, P.M., "Implicit Finite-Difference Computations of Unsteady Transonic Flow About Airfoils," *AIAA Journal*, Vol. 15, Dec. 1977, pp. 1728-1735.

[9]Yang, T.Y., Guruswamy, P., Striz, A.G., and Olsen, J.J., "Flutter Analysis of a NACA 64A006 Airfoil in Small Disturbance Transonic Flow," *Journal of Aircraft*, Vol. 17, 1980, pp. 225-232.

[10]Edwards, J.W., Bennett, R.M., Whitlow, Jr., W., and Seidel, D.A., "Time-Marching Transonic Flutter Solutions Including Angle-of-Attack Effects," *Proceedings of the 23rd AIAA/SDM Conference*, New Orleans, La., May 1982.

[11]Taylor, R.F., Bogner, F.K., and Stanley, E.C., "A Stability Prediction Method for Nonlinear Aeroelasticity," *Proceedings of the 21st AIAA/SDM Conference*, Seattle, Wash., May 1980.

[12]Bland, S.R. and Edwards, J.W., "Airfoil Shape and Thickness Effects on Transonic Airloads and Flutter," *Proceedings of the 24th AIAA/SDM Conference*, Lake Tahoe, Nev., May 1983.